Cell Reports, Volume *27*

Supplemental Information

TCF1 and LEF1 Control Treg Competitive Survival and Tfr Development to Prevent Autoimmune Diseases

Bi-Huei Yang, Ke Wang, Shuo Wan, Yan Liang, Xiaomei Yuan, Yi Dong, Sunglim Cho, Wanqing Xu, Kristen Jepsen, Gen-Sheng Feng, Li-Fan Lu, Hai-Hui Xue, and Wenxian Fu

Fig.S1-related to Figure 1

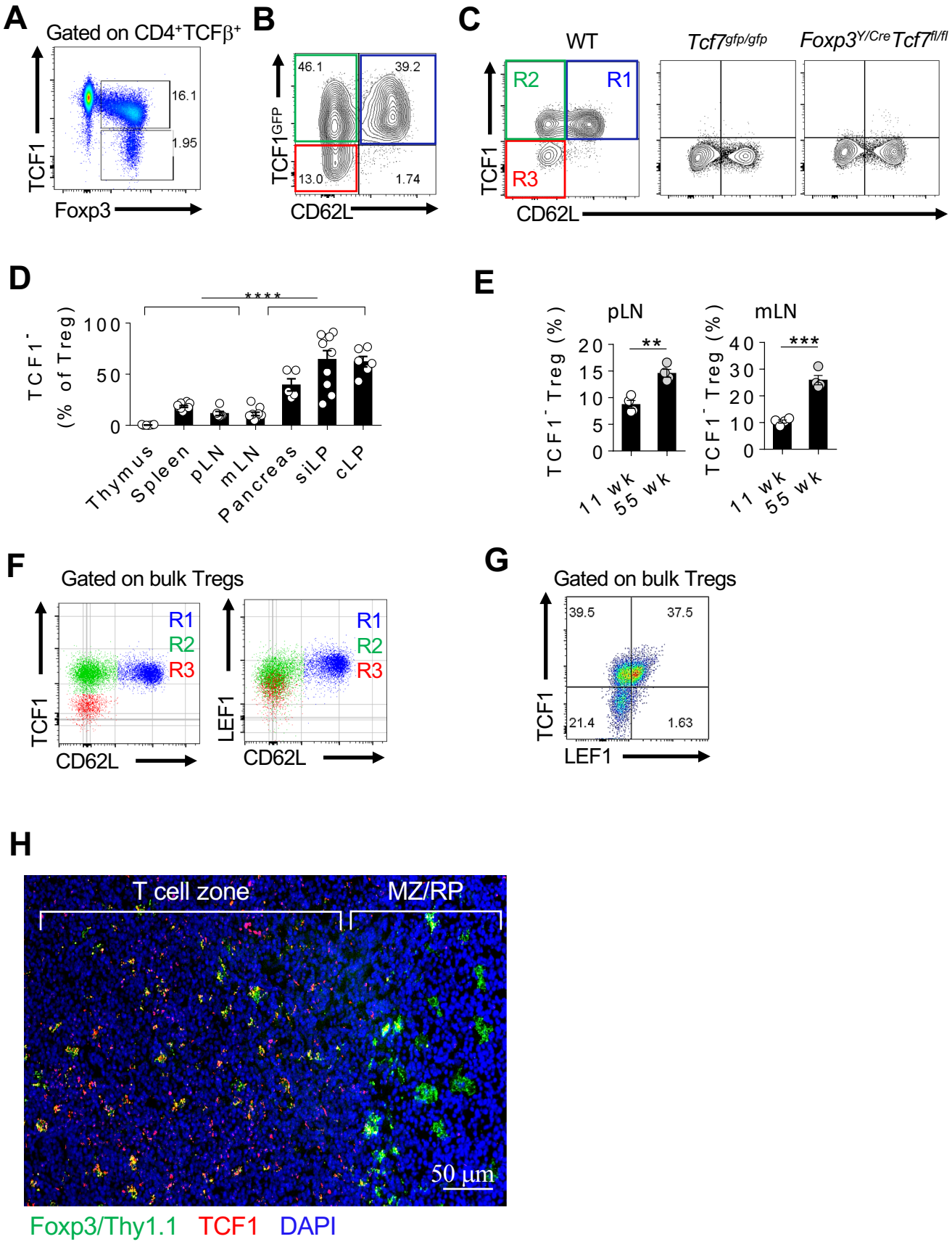

Fig. S1-related to Figure 1. The expression of TCF1 and LEF1 in peripheral Treg cells.

(A) Flow cytometric plot of Foxp3 and TCF1 expression in splenic $CD4^+$ T cells.

(B) Flow cytometric analysis of TCF1(GFP) and CD62L expression in Treg cells of $Foxp3^{Thy1.1}Tcf7^{+/gfp}$ reporter mice.

(C) Flow cytometric analysis of TCF1 and CD62L expression in Treg cells from WT, $Tcf7^{gfp/gfp}$ and $Foxp3^{Y/Cre}Tcf7^{fl/fl}$ mice.

(D) The percentages of $TCF1^-$ Tregs in central, peripheral lymphoid organs and non-lymphoid tissues. Pancreas data were from 10-12 wks old NOD mice.

(E) Graphic summary of $TCF1^-$ Treg percentages in pLNs and mLNs of 11-wk and 55-wk old B6 mice.

(F) Flow cytometric profiles of TCF1/CD62L and LEF1/CD62L plots in Treg cells. anti-TCF1 staining shows a better distinguishment of R2 and R3 than that by anti-LEF1.

(G) Flow cytometric plot of TCF1 and LEF1 expression in Treg cells.

(H) Immunostaining of frozen splenic section depicting the distributions of $TCF1^+$ and $TCF1^-$ Treg cells. T cell zone can be identified by the dense expression of TCF1 (red).

The data are representative of more than three independent experiments. Shown are mean ± s.e.m. **, $p<0.01$; ***, $p<0.001$ (two-tailed unpaired Student's *t* test). wk, week. pLN, peripheral (cervical, axillary, brachial and inguinal) lymph nodes; mLN, mesenteric lymph nodes; siLP, small intestinal lamina propria; cLP, colon lamina propria.

Fig. S2-related to Fig. 2

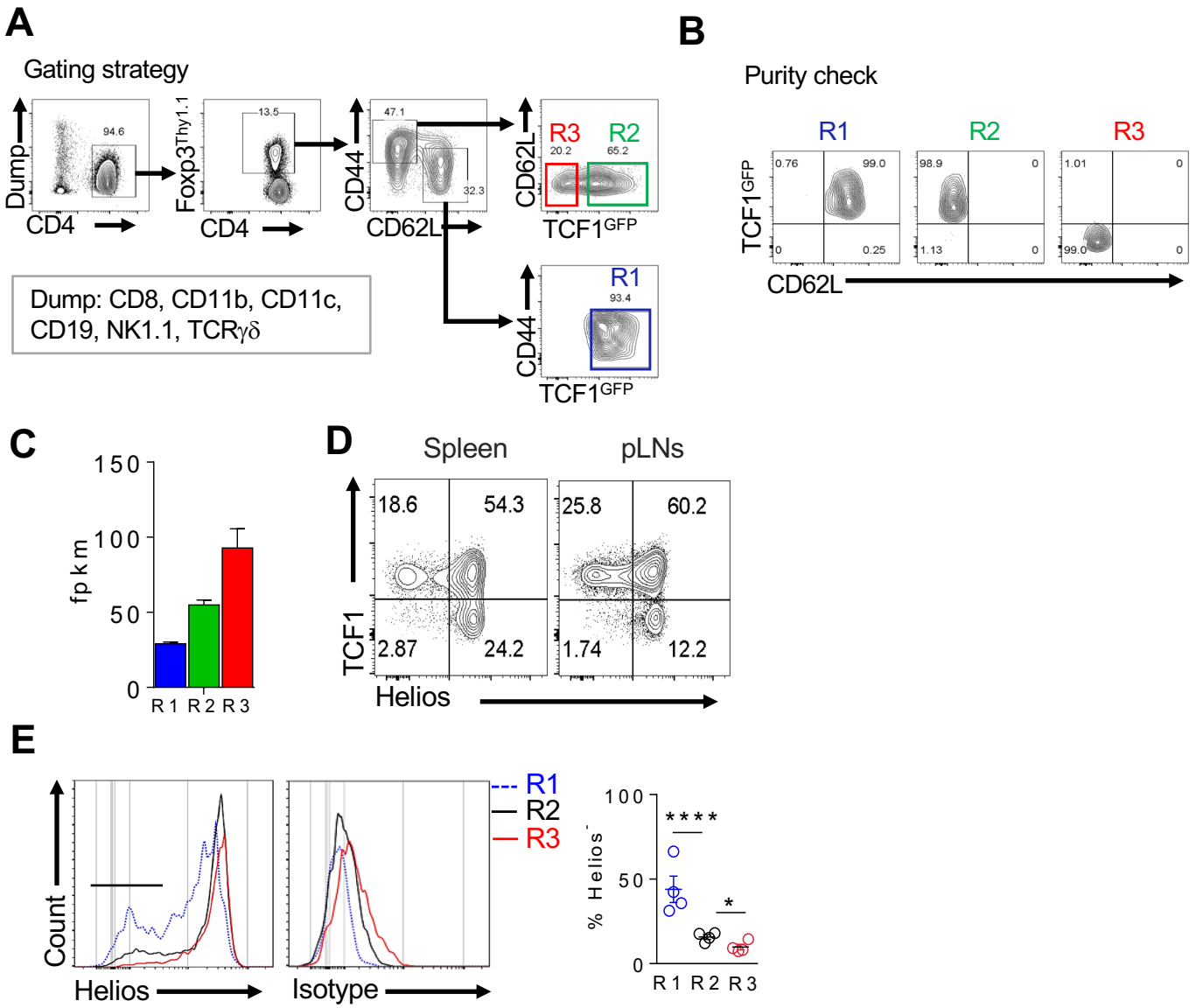

Fig. S2-related to Figure 2. Characterization of rTreg, aTreg and eTreg subsets.

(A) Gating Strategy for the R1, R2, R3 subset for FACS sorting.
(B) Purity check for sorted subpopulations.
(C) Expression of *Ikzf2* in r-, a-, and e- Treg subsets determined by RNA-seq analysis.
(D) Expression profile of Helios and TCF1 in Tregs in spleen and pLNs.
(E) Histogram of Helios expression in r-, a-, and e- Treg subsets. Note that a substantial proportion of rTregs were Helios$^-$. This proportion was significantly lower in aTregs and eTregs.

The data are representative of three independent experiments (C-E). **, $p<0.05$; ****, $p<0.0001$* (two-tailed unpaired Student's *t* test). pLN, peripheral (cervical, axillary, brachial and inguinal) lymph nodes; fpkm, fragments per kilobase of transcript per million mapped reads.

Fig. S3-related to Fig. 3

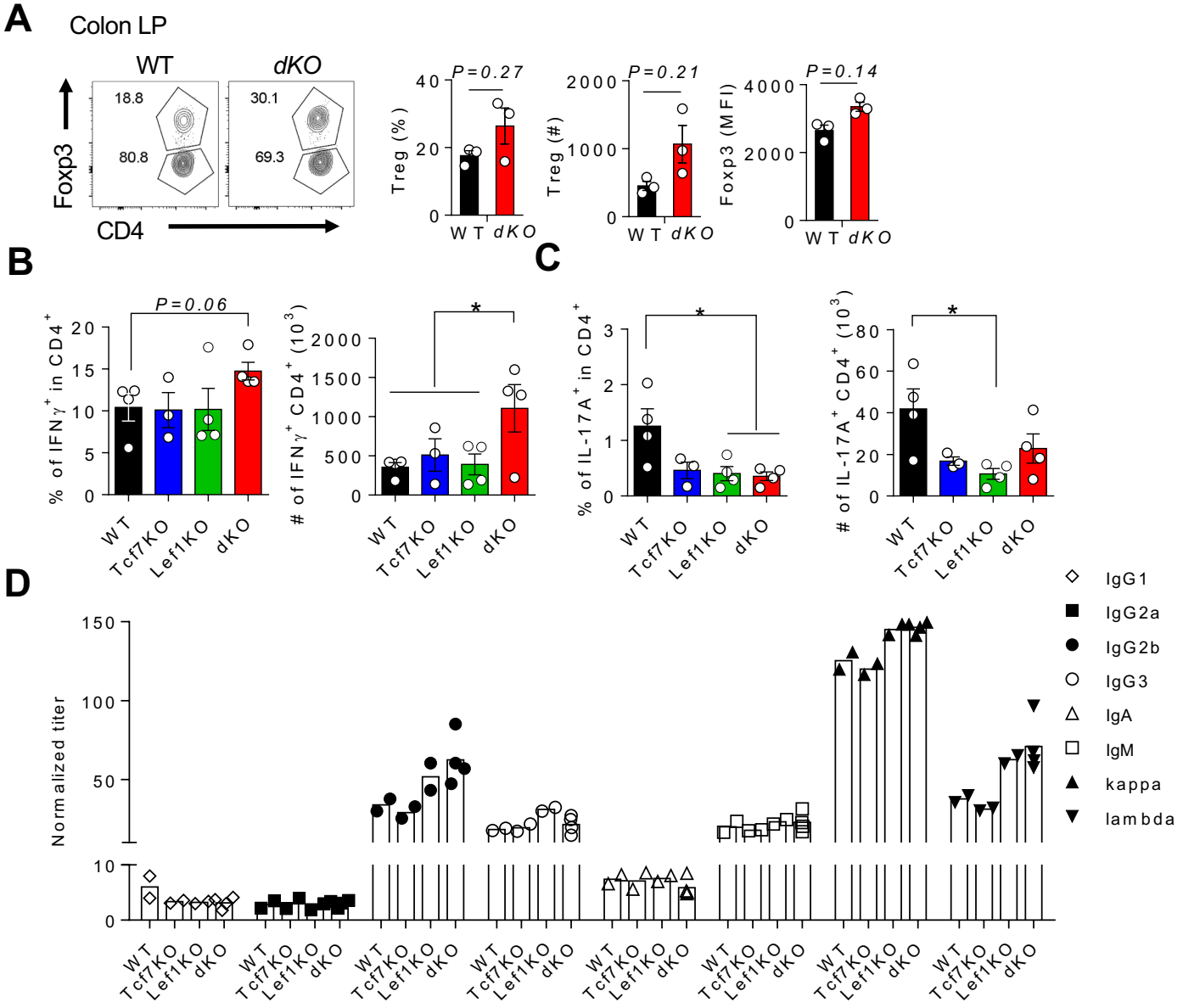

Fig. S3-related to Figure 3. Characterization of *Tcf7KO, Lef1KO* and *Tcf7/Lef1 dKO* mice.

(A) The percentages and numbers of Treg cells in colonic lamina propria (LP) of *dKO* and littermate control WT mice. The data are pooled of 3 mice in each group

(B) Flow cytometric analysis of the percentages and numbers of IFNγ-producing $CD4^+$ cells from spleen of mice as indicated.

(C) Flow cytometric analysis of the percentages and numbers of IL-17A-producing $CD4^+$ cells from spleen of mice as indicated.

(D) Isotype of immunoglobulin subclasses in the sera from indicated mice. The data are pooled of n= 2-4 mice in each group. LP, lamina propria.

The data are representative of three independent experiments. Shown are mean ± s.e.m. *, $p<0.05$ (two-tailed unpaired Student's *t* test).

Fig. S4-related to Fig. 4

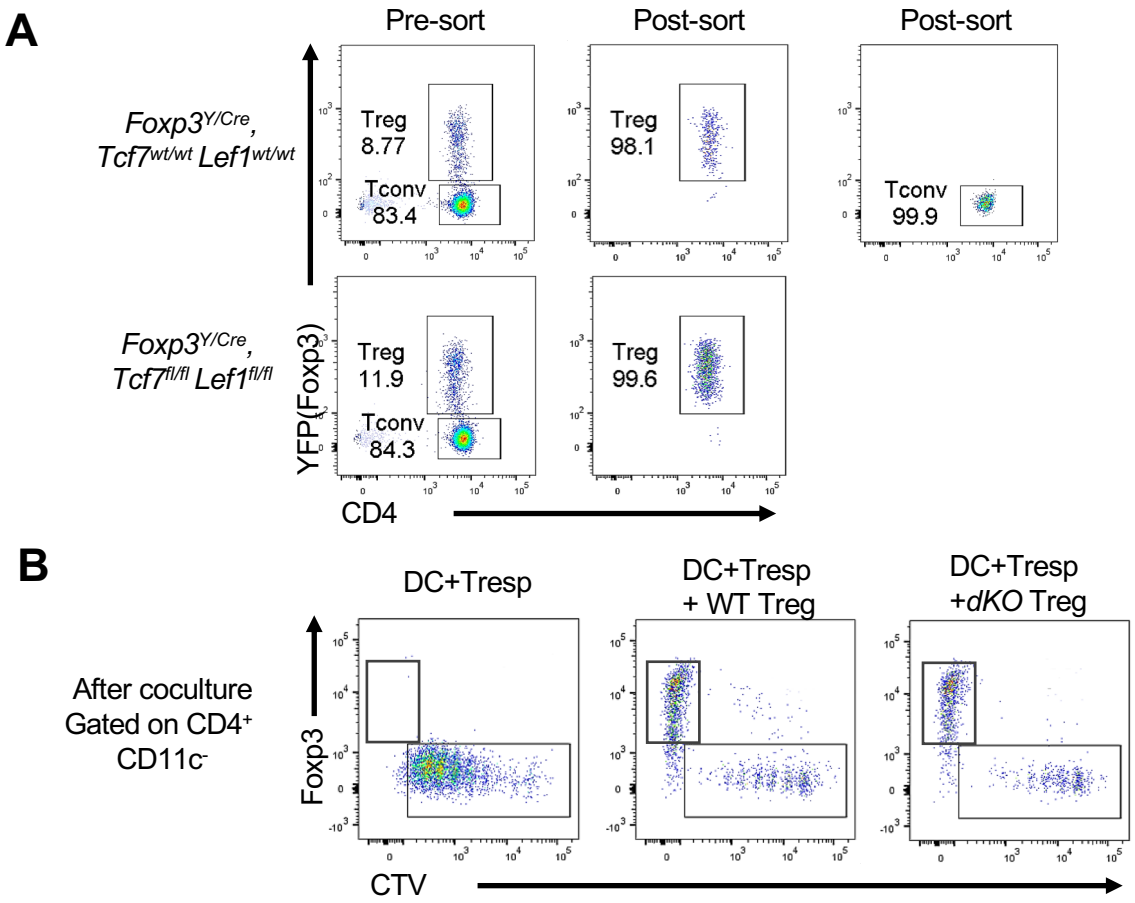

Fig. S4-related to Figure 4. Cell sorting and culture for *in vitro* Treg suppressive assays.
(A) Purity check for sorted Treg and Tresp cells for *in vitro* suppression assays.
(B) Representative FACS plots after coculture to show the presence of Treg cells and the dilution of CTV.

Fig. S5-related to Fig. 5

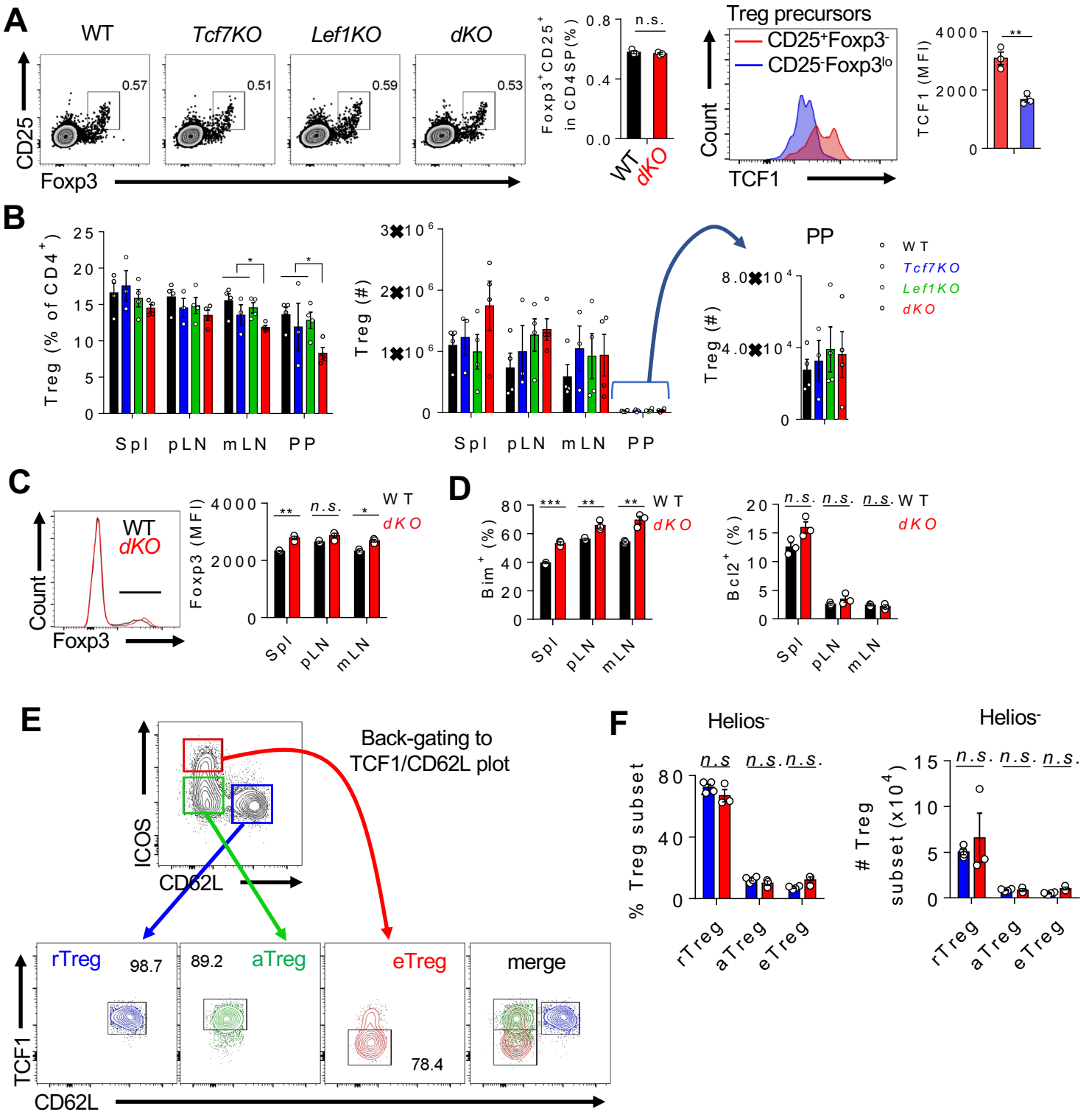

Fig. S5-related to Figure 5. Phenotypic and functional properties of Tregs with Foxp3-Cre mediated ablation of *Tcf7*, *Lef1* or both.

(A) (left) Flow cytometric analysis of CD25 vs. Foxp3 expression in CD4SP thymocytes. (right) The expression levels of TCF1 in two types of thymic Treg precursors.
(B) The numbers and percentages of Treg cells among $CD4^+$ T cells in spleen (Spl), pLN, mLN and Peyer's patches (PP) of the mice with indicated genotypes.
(C) Flow cytometric analysis of Foxp3 expression in $TCR\beta^+$ $CD4^+$ cells from indicated organs.
(D) Flow cytometric analysis of Bim and Bcl2 expression in *ex vivo* WT and *dKO* Tregs.
(E) Gating strategy using ICOS/CD62L plot to separate r-, a- and e- Treg cells. The ICOS/CD62L plot is over 80% overlapped with the TCF1/CD62L plot defined in Figure 1.
(F) (related to Fig. 5G) The percentages and numbers of each Treg subset in $Helios^-$ Treg compartment.

The data are pooled of two experiments with n=3-4 mice in each group. The *P* values were calculated using two-tailed unpaired Student's *t* test. *, $p<0.05$; **, $p<0.01$; ***, $p<0.001$; ****, $p<0.0001$; *n.s.*, non-significant.

Fig. S6-related to Figure 6

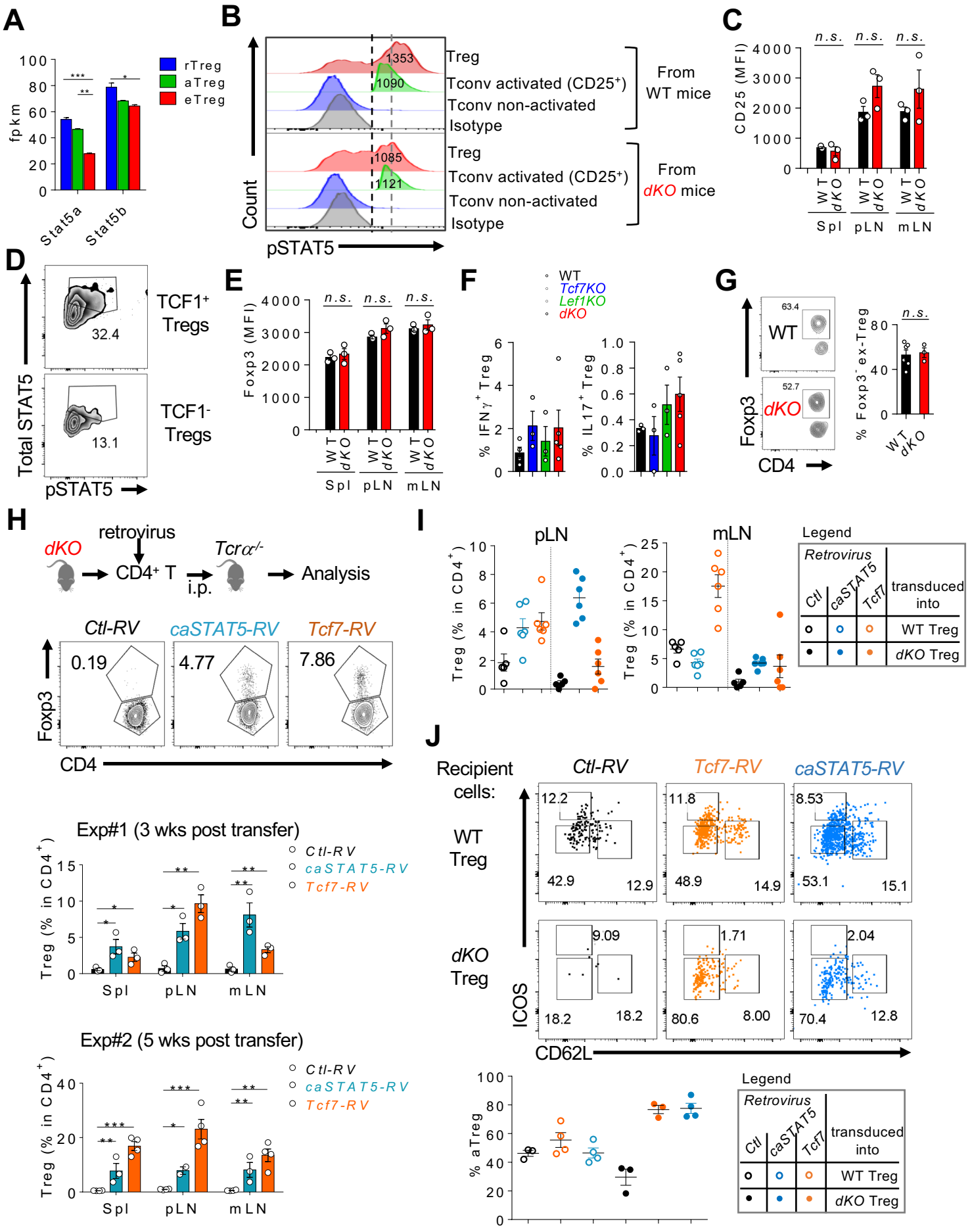

Fig. S6-related to Figure 6. Phenotypic and functional properties of Tregs with Foxp3-Cre mediated ablation of *Tcf7*, *Lef1* or both.

(A) The expression of *Stat5a* and *Stat5b* in WT and *dKO* Tregs measured by RNA-seq.
(B) Histograms of pSTAT5 in indicated cell types. Numbers are the MFI of pSTAT5.
(C) MFI of CD25 protein in WT and *dKO* Tregs from spleen, pLNs and mLNs.
(D) Flow cytometric analysis of the expression of total STAT5 protein and pSTAT5 in fractionated TCF1$^+$ and TCF1$^-$ Tregs.
(E) MFI of Foxp3 protein in WT and *dKO* Tregs from spleen, pLNs and mLNs.
(F) Flow cytometric analysis of inflammatory cytokine production in *ex vivo* WT and *dKO* Tregs.
(G) Stability of dKO Tregs. Highly-purified Treg cells were sorted from pooled spleen and pLNs of either WT (CD45.1$^+$CD45.2$^+$ *Foxp3*$^{y/Cre}$) or *dKO* mice (CD45.1$^-$CD45.2$^+$ *Foxp3*$^{y/Cre}$ *Tcf7*$^{fl/fl}$ *Lef1*$^{fl/fl}$), mixed and co-transferred with Tconvs isolated from CD45.1$^+$CD45.2$^-$ mice into recipient *Tcrα*$^{-/-}$ mice. The expression of Foxp3 in each type of donor Tregs were analyzed 3 weeks later.
(H) Rescue assays under non-competitive conditions. Splenic CD4$^+$ T cells from *dKO* mice were MACS enriched and transduced with retroviruses expressing *Tcf7*, or *caSTAT5, i.p.* transferred into *Tcrα*$^{-/-}$ mice and analyzed 3 or 5 weeks later. FACS and statistical data showing the percentages of Treg cells reconstituted from each type of donor cells in spleen, pLNs and mLNs.
(I) Rescue assays under competitive conditions (related to Fig. 6I). Splenic CD4$^+$ T cells from congenic WT or *dKO* mice were MACS enriched, mixed (1:1) and transduced with retroviruses expressing *Tcf7*, or caSTAT5, *i.p.* transferred into *Tcrα*$^{-/-}$ mice and analyzed 3 weeks later. Shown are Treg reconstitution in pLNs and mLNs in each condition as described in the insert legend.
(J) The ICOS/CD62L plot was used to show the compositions of reconstituted Treg pool under each condition as indicated in the experiments described in Fig. 6I.

The data are from one experiment with two replicates for each Treg subsets (A); representative of three (B, D, F); two (C, E, G-J) independent experiments. The *P* values were calculated using two-tailed unpaired Student's *t* test. *, *p<0.05;* **, *p<0.01;* ***, *p<0.001; n.s., non-significant*. *RV*, retrovirus; *Ctl*, control; wk, week. fpkm, fragments per kilobase of transcript per million mapped reads.

Fig. S7-related to Figure 7

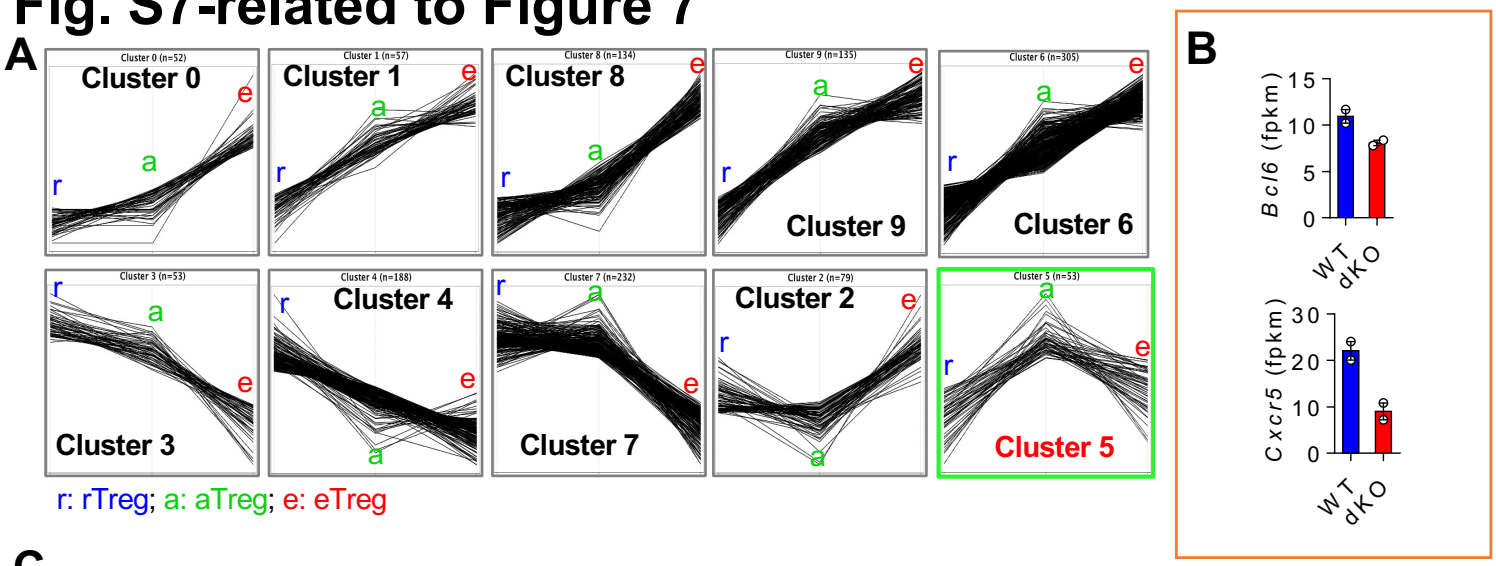

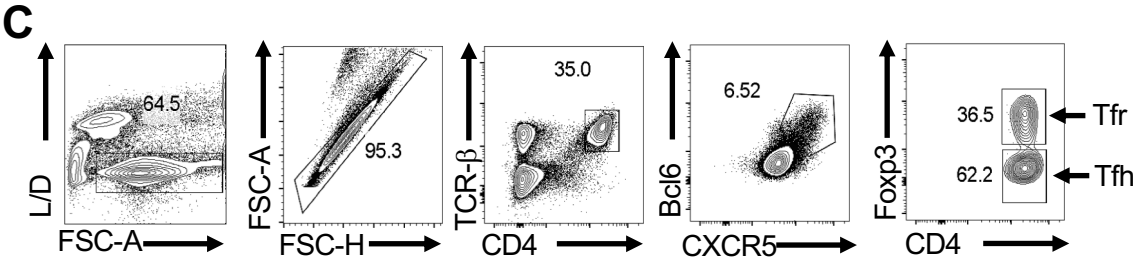

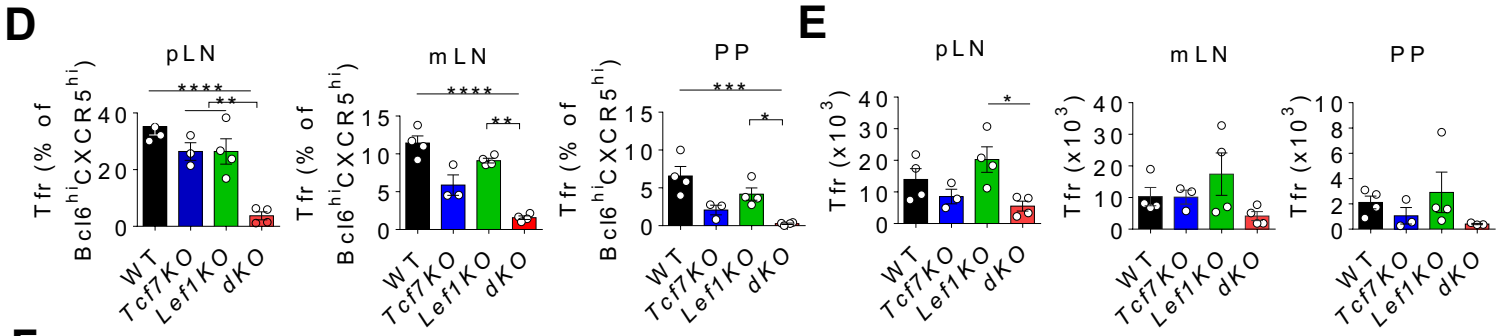

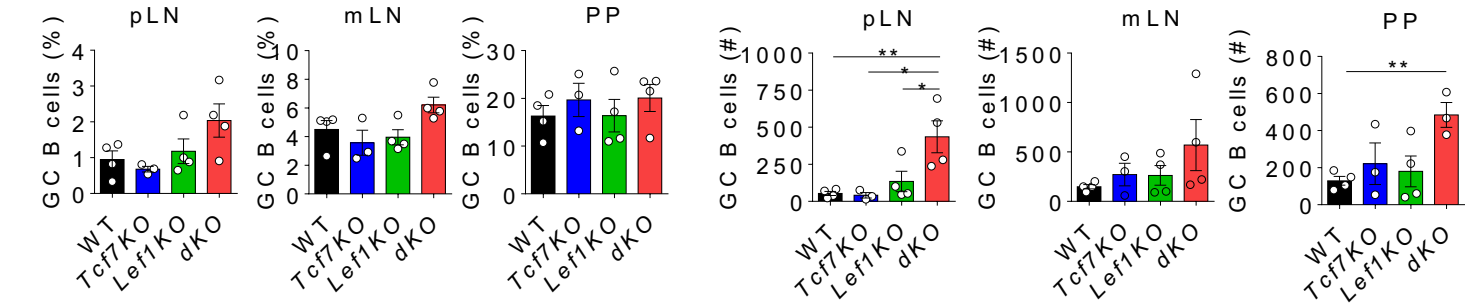

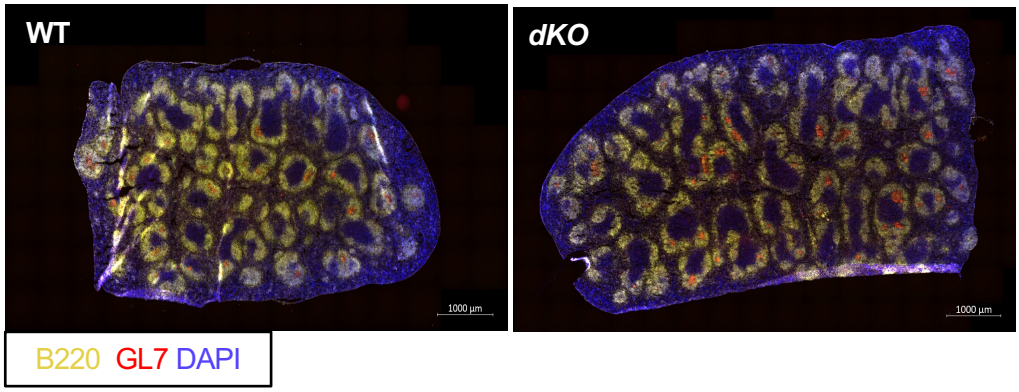

Fig. S7-related to Figure 7. Characterization of mice with Treg-specific ablation of *Tcf7*, *Lef1* or both.

(A) *k*-means clustering analysis of differentially-expressed (DE) genes across the transcriptomes of the r-, a- and e-Treg subsets. The names of the genes in cluster 5 were highlighted. Also see Table S5.
(B) The expression of *Bcl6* and *Cxcr5* in *dKO* and WT Tregs measured by RNA-seq.
(C) Gating strategy of to show Tfh and Tfr simultaneously in the same plot.
(D) The percentages Tfr cells in $CD4^+$ $Bcl6^{hi}$ $CXCR5^{hi}$ cells in pLNs, mLNs and Peyer's patches (PP).
(E) The total numbers of Tfr cells in pLNs, mLNs and PP.
(F) The percentages of GC B cells in $B220^+$ cells in pLNs, mLNs and PP.
(G) The total numbers of GC B cells in pLNs, mLNs and PP.
(H) Microscopic images of the spleen from $Tcf7^{wt/wt}Lef1^{wt/wt}$; $Foxp3^{cre}$ (WT) and $Tcf7^{fl/fl}Lef1^{fl/fl}$;$Foxp3^{cre}$ (*dKO*) mice, showing the staining of B220, GL7 and DAPI.

The data are representative of two replicates for each Treg subsets (A-B); or two experiments with 3-4 mice in each group (C-H). The *P* values in (D-G) were calculated using two-tailed unpaired Student's t test. *, $p<0.05$; **, $p<0.01$; ***, $p<0.001$; ****, $p<0.0001$. fpkm, fragments per kilobase of transcript per million mapped reads.